



90 % of vPP was converted to petroleum, while PE waste was converted to wax, gasoline blends, or diesel (Jin et al., 2021).

In a study by Chen et al. (2019), vPP was degraded at 450 °C for 0.5 to 4 h. The maximum yield of the oil phase (91 %), which was similar in composition to petroleum, was obtained after 1 h. The resulting gas phase consisted mainly of C<sub>3</sub> and C<sub>4</sub> hydrocarbons. In another study by Seshasayee and Savage (2020), conducted in a microreactor, a yield of 15 % of the oil phase, which was a mixture of gasoline, diesel, and kerosene, was reported after hydrothermal decomposition of vPP at 450 °C after 1 h. A study of the decomposition of waste PP by Jin et al. (2021) showed that at 450 °C and a time of 1 h, 80 % of the oil phase was formed. In our study, at a degradation temperature of 450 °C and a time of 1 h, 85 % of the oil phase was formed, which consisted mainly of aromatic and alicyclic compounds. The gas phase is dominated by C<sub>3</sub> hydrocarbons. It is difficult to compare the results of the decomposition of vPP and rPP in different previously published works because the process parameters (heating rate, material-to-water ratio) and the separation technique used were different. In addition, different analytical techniques and methods were used to present the results, which makes it difficult to properly compare the chemical composition of the resulting products and evaluate the future potential uses of these products. Therefore, in order to compare the results for vPP and rPP and to evaluate the influence of the material on the decomposition pathways, it is important to perform a decomposition study at specified process and technical characteristics (reactor size, heating rate, ...) equal for both materials.

The main objective of this study was to compare the hydrothermal degradation rate of recycled polypropylene (rPP) and virgin polypropylene (vPP) under the same conditions. In addition, the products (oil and gas phases) were characterised by GC/MS and their composition was compared. The total carbon (TC) in water was also used to evaluate the transfer of the compounds into the water phase during the degradation itself and served as an indicator of the contamination of the water used.

## 2. Material and methods

This section describes the material characterization methods, hydrothermal degradation process, and analytical procedures for two polypropylene samples, vPP (uncolored) and rPP (grey). vPP and rPP in the form of pallets were supplied by the local plastic manufacturing company.

Hydrothermal decomposition of polypropylene was carried out in a high-temperature, high-pressure batch reactor (Parr instruments) at a temperature of 450 °C and a reaction time of 15 to 240 min. The reactor consisted of a reaction vessel, a gas inlet and outlet valve system, a heating wire with a temperature controller, a magnetic mixer, a thermocouple, and a pressure gauge. First, the proper amount of material and deionised water was added to the reactor to achieve a material-to-water ratio of 1:10 (g:mL), and a magnetic stirrer was added. The reactor was closed and purged three times with nitrogen through the valve system. Then the valve system was closed and heating started at a rate of about 20 °C/min. The reaction time started at the moment when the temperature reached 450 °C. After the desired reaction time was reached, the reactor was quenched in cold water to lower the temperature as quickly as possible. When the reactor temperature reached room temperature, the gas phase formed was collected in gas sample bags (Tedlar) for further analysis. The water-oil mixture remaining in the reactor was then filtered by vacuum filtration to separate the solid phase. The reactor and filter paper were washed with dichloromethane (DCM) to avoid losses. The filter paper was dried at 70 °C and then weighed to determine the solid phase. The aqueous and oil phases were then separated in a separatory funnel. The DCM from the oil phase was removed using a rotary evaporator under vacuum. The aqueous and oil phases were stored in glass vials in the refrigerator for further analysis. The yields of the oil and solid phases were calculated by Eq(1) and Eq(2)

$$\hat{U}^o = L \frac{m^o}{m^o + m^s}; \quad (1)$$

$$\hat{U}^s = L \frac{m^s}{m^o + m^s}; \quad (2)$$

where  $\hat{U}^o$  and  $\hat{U}^s$  are yields of oil and solid phase,  $m^o$  and  $m^s$  are weights of oil and solid phase and  $m^o + m^s$  is the weight of material put in the reactor. The yield of gas phase was calculated by Eq.3

$$\hat{U}^g = L \left( \frac{m^g}{m^o + m^s} \right); \quad (3)$$

where  $\hat{U}^g$  is the yield of gas phase.

The composition of the gas and oil phases was determined using the GC-MS apparatus, which consists of the Shimadzu GC-2010 gas chromatograph and the Shimadzu GC-MS 2010 QC Ultra mass selective detector. Analyses were done in triplicate. Gas phase compounds were separated on a HP-PLOTQ capillary column

(dimensions 30 m x 0.32 mm i.d.; 20  $\mu\text{m}$  film thickness) with helium as the carrier gas (0.87 mL/min). The separation was achieved using a temperature gradient as follows: 35  $^{\circ}\text{C}$  held for 5 min, then increased by 10  $^{\circ}\text{C}/\text{min}$  to 80  $^{\circ}\text{C}$ , held for 1 min, then increased to 200  $^{\circ}\text{C}$  with 5  $^{\circ}\text{C}/\text{min}$  and held at final temperature for 5 min. Samples were injected at 250  $^{\circ}\text{C}$  in split mode at a ratio of 1:100. The transfer line temperature was 250  $^{\circ}\text{C}$  (Kotnik et al., 2020). Oil phase compounds were separated using a HP-1 capillary column (dimensions 30 m x 0.25 mm i.d.; 25  $\mu\text{m}$  film thickness) with helium as the carrier gas (1 mL/min). The injection of samples was performed by splitless mode. The separation was achieved using temperature gradient as follows: 40  $^{\circ}\text{C}$  held for 1 min, then increased by 10  $^{\circ}\text{C}/\text{min}$  to 180  $^{\circ}\text{C}$ , and at 5  $^{\circ}\text{C}/\text{min}$  to 230  $^{\circ}\text{C}$  and held at the final temperature for 5 min. The injector port and transfer line temperatures were set at 250  $^{\circ}\text{C}$ . Mass detector conditions for both methods were: electronic impact (EI) mode at 70 eV; source temperature 250  $^{\circ}\text{C}$ ; scanning rate 1 scan/s; mass acquisition range 35-500 m/z (mass divided by charge number). Identification of all compounds was based on comparison of their retention times and mass spectra according to the NIST library (2014).

Finally, the determination of TC in the water phase was performed using the Shimadzu TOC-L instrument. The concentration of total carbon in the aqueous phase after hydrothermal degradation of vPP and rPP in SCW was calculated using the calibration curve of sodium hydrogen phthalate with a concentration range from 10 to 1,000 ppm. All measurements were performed in triplicate.

### 3. Results and discussion

The results of the yield of hydrothermal decomposition presented in Figure 1 show that the main product is the oil phase, the yield of which ranges from 56.2 $\pm$ 1.2 % to 96.9 $\pm$ 2.2 %. After 15 min of decomposition, some unreacted material remains, namely 8.5 $\pm$ 0.3 % for vPP and 10.3 $\pm$ 0.3 % for rPP. The maximum oil phase yield was reached after 30 min of degradation and was slightly higher for vPP degradation (96.9 $\pm$ 2.2 %) than for rPP degradation (94.5 $\pm$ 2.0 %). In general, the oil phase yield was higher for vPP degradation than for rPP degradation at all reaction times, which can be expected since rPP contains more additives and impurities that are most likely to form a solid residue instead of oil. As the reaction time increased, the oil phase yield started to decrease, while the gas phase yield started to increase. After 240 min, the oil yield in vPP degradation is about 10 % higher than that in rPP degradation, while the gas phase yield is almost the same, 33.0 $\pm$ 1.8 % for vPP degradation and 32.8 $\pm$ 1.7 % for rPP degradation. The difference in oil phase yield is reflected in the increase in solid residue yield. After 240 min of decomposition, this was 11.1 $\pm$ 0.3 % for rPP degradation, while only 0.9 $\pm$ 0.1 % solid residue was obtained for vPP degradation after the same time.

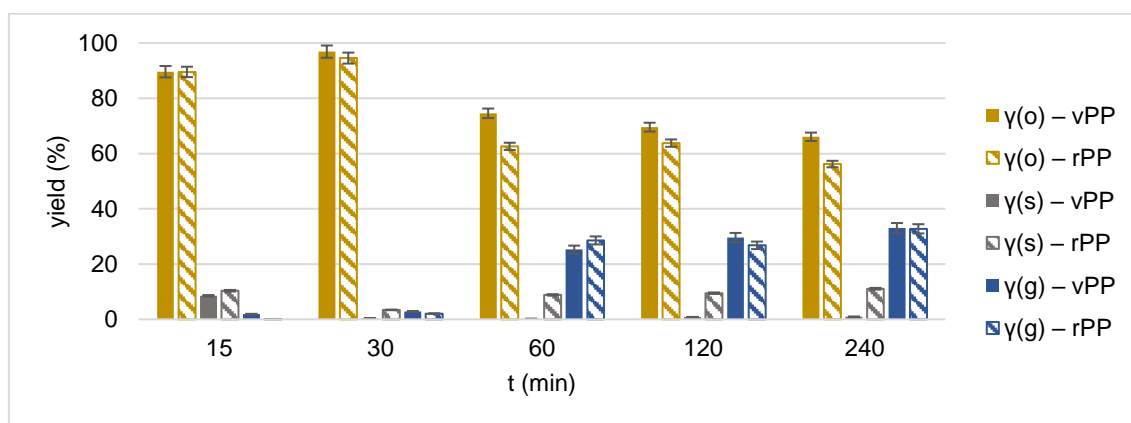


Figure 1: Yields of oil  $y(o)$ , solid  $y(s)$  and gas  $y(g)$  phase after the hydrothermal decomposition of vPP and rPP

The results obtained in this study are in agreement with the literature (Chen et al., 2019), where the maximum of the oil phase (91 %) is reached after 30 min in the degradation of vPP at 450  $^{\circ}\text{C}$ . They also report an increase in gas-phase yield and a decrease in oil-phase yield with increasing reaction time from 1 h to 4 h. The increase in solid residue yield during the decomposition of rPP with increasing reaction time can be attributed to the increased formation of char from the additives and dyes present in rPP, which can account for up to 5 % of the material (Hahladakis et al., 2018), while these are less present in vPP, so the increase in solid residue yield during the decomposition of vPP is not as significant.

### 3.1 Oil phase composition

The chemical composition of the oil phase after hydrothermal degradation was determined by GC/MS. The detected components were divided into different hydrocarbon groups, namely saturated and unsaturated aliphatic hydrocarbons, alicyclic hydrocarbons, aromatic hydrocarbons and alcohols, as shown in Figure 2. Since some ketones and organic acids were also detected, these are listed among the others. Figure 2a shows the composition of the oil phase after the degradation of vPP. It was found that after a short reaction time, the oil was mainly composed of unsaturated aliphatic hydrocarbons and alicyclic compounds. After 15 min of vPP degradation, the oil contained  $52.75\pm 1.00\%$  alkenes and  $24.77\pm 0.50\%$  alicyclics. A similar composition, in which olefins were most abundant in the oil phase after hydrothermal degradation at  $400\text{ }^\circ\text{C}$  for 60 min, has been reported previously (Zhao et al., 2021). With increasing reaction time, it was observed that the concentration of alkenes and alicyclics decreased drastically, while the concentration of aromatic compounds increased. This can be mainly attributed to the process of cyclization of unsaturated aliphatic hydrocarbons to alicyclics, which are then further processed to aromatic compounds by the process of dehydrogenation (Chen et al., 2019). After 240 min of decomposition, alkenes are no longer present in the oil and only  $9.32\pm 0.19\%$  alicyclics remain. In contrast, the concentration of aromatic hydrocarbons increases to  $88.84\pm 1.95\%$ . The concentration of alkanes and alcohols reaches a maximum after 30 min of decomposition and then starts to decrease.

The composition of the oil after rPP degradation, as shown in Figure 2b, follows similar principles to vPP degradation. The difference is that in rPP degradation, aromatic compounds are more represented with  $12.71\pm 0.36\%$  after 15 min of degradation. It can also be seen that the concentration of aromatic compounds increases faster with increasing reaction time than in vPP degradation. For example, the concentration of aromatic compounds after 120 min of rPP degradation is already  $80.81\pm 1.78\%$ , while the concentration of aromatic compounds in vPP degradation is only  $67.33\pm 1.48\%$ . The final composition of the oil after 240 min of degradation is very similar for vPP and rPP. From the results, it can be concluded that the aromatization process from alkenes and alicyclics is faster in the degradation of rPP than in the degradation of vPP. "The compounds contained in the oil may be of interest to the market, and by changing the reaction time, the reaction can be directed towards the formation of the desired compounds."

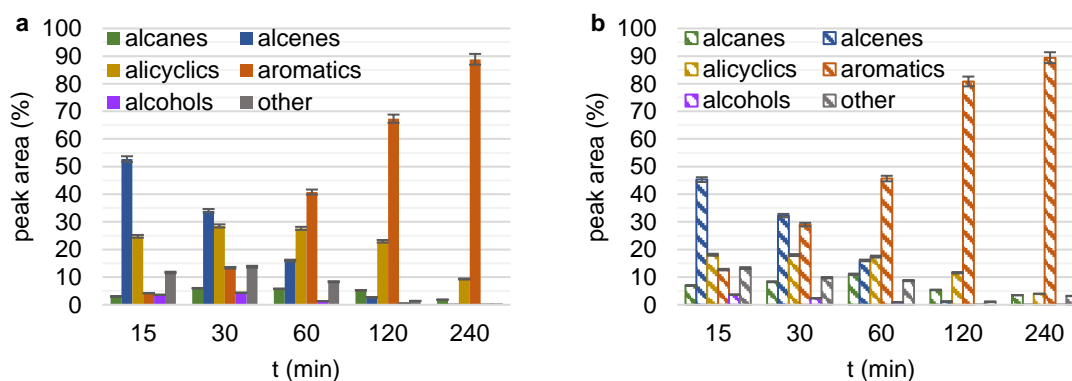


Figure 2: Composition of oil phase after the hydrothermal decomposition of (a) vPP and (b) rPP

### 3.2 Gas phase composition

The chemical composition of the gas phase after the decomposition of vPP and rPP was also determined by GC/MS and is shown in Figure 3. In both cases, the gas phase consisted of  $\text{CO}_2$  and saturated and unsaturated  $\text{C}_1\text{-C}_6$  aliphatic hydrocarbons. The composition of the gas phase is similar for both the hydrothermal decomposition of vPP and the decomposition of rPP.  $\text{C}_2\text{-C}_3$  hydrocarbons predominate, accounting for more than 50 % of the gas phase. It can be observed that the concentration of  $\text{C}_3$  hydrocarbons decreases with increasing reaction time. For example, in the degradation of vPP, the concentration decreased from  $44.31\pm 0.89\%$  to  $36.68\pm 0.73\%$ , and in the degradation of rPP, the concentration decreased from  $43.63\pm 0.87\%$  to  $36.33\pm 0.76\%$ . In general, the concentration of  $\text{C}_5$  and  $\text{C}_6$  hydrocarbons decreases with increasing reaction time, which can be attributed to the decomposition of longer hydrocarbons into shorter hydrocarbons, which has also been reported for gasification of PP at high temperatures ( $500\text{ }^\circ\text{C}$ ) in supercritical water (Bai et al., 2020). Conversely, it is observed that the concentration of  $\text{C}_2$  hydrocarbons and methane increases with increasing reaction time, so that in the degradation of vPP, the concentration of methane increases from  $3.93\pm 0.08\%$  to  $7.36\pm 0.14\%$ , while the concentration of  $\text{C}_2$  hydrocarbons increases from  $26.20\pm 0.55\%$  to  $29.29\pm 0.62\%$ . The

increase in the concentration of methane and C<sub>2</sub> hydrocarbons is slightly less pronounced in the decomposition of rPP. The concentration of CO<sub>2</sub> produced is slightly higher in the decomposition of rPP, ranging from 2.04±0.04 % to 1.35±0.03 % than in the decomposition of vPP, where it ranges from 0.41±0.01 % to 0.12±0.01 %. If we look more closely at the composition of the individual hydrocarbon groups, we find that after 15 min of decomposition, the unsaturated hydrocarbons dominate, which are then converted into saturated hydrocarbons by a hydrogenation process as the reaction time increases. For example, in the case of C<sub>3</sub> hydrocarbons, after 15 min of VPP decomposition, 15.80±0.32 % propane and 28.51±0.57 % propene are present, and after 240 min of decomposition, only 1.63±0.03 % propene is present, and the propane concentration increases to 35.02±0.70 %. C<sub>3</sub> hydrocarbons can be used for the re-synthesis PP, and ethane is a valuable product used in many chemical synthesis processes (Chen et al., 2019).

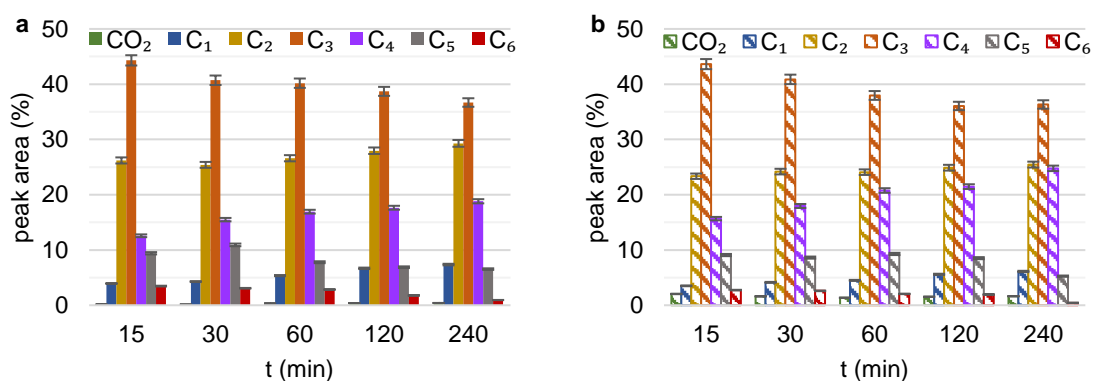


Figure 3: Composition of gas phase by the number of C-atoms after the hydrothermal decomposition of (a) vPP and (b) rPP

### 3.3 Total carbon (TC) content in aqueous phase

From the TC concentrations in the aqueous phase shown in Table 1, it is evident that these are much higher for rPP degradation than for vPP degradation at short reaction times. After 15 min of degradation, the TC is 4,394±92 mg/L for rPP degradation, while it is 2,604±49 mg/L for vPP degradation. The higher TC concentration for rPP degradation can be mainly attributed to the additives present in rPP, which are mainly organic dyes that transfer to the aqueous phase. It can be observed that TC decreases with increasing reaction time. The decrease of TC with increasing reaction time is much more pronounced in the degradation of rPP, which is 1,760±37 mg/L after 240 min of degradation time, which is less than the TC in the degradation of vPP, which is 2,079±40 mg/L with the same degradation time. The decrease in the concentration of TC can be explained by the fact that the components in the aqueous phase are subjected to a gasification process with longer reaction times (Čolnik et al., 2022). TC concentration can be a valuable indicator of water pollution, and the results show that the water pollution for vPP decomposition is almost constant, as for the rPP degradation, the water pollution is reduced with increasing reaction time.

Table 1: Total carbon (TC) concentration in aqueous phase after hydrothermal decomposition of vPP and rPP.

t [min]	15	30	60	120	240
TC – vPP (mg/L)	2,604 ± 49	2,713 ± 52	2,846 ± 54	2,305 ± 44	2,079 ± 40
TC – rPP (mg/L)	4,394 ± 92	3,384 ± 71	3,082 ± 65	2,978 ± 63	1,760 ± 37

## 4. Conclusion

This study presents the results of a comparison of the hydrothermal decomposition of virgin and recycled PP, a commonly used plastic. The results show that the decomposition products differ in chemical composition depending on which material was used for decomposition. Therefore the results indicate the importance of a comparative study, since the technique is likely to be applied to different polypropylene wastes and the results obtained with virgin materials could be misleading. A slightly higher yield of the oil phase was observed for hydrothermal degradation of vPP than for degradation of rPP, as the maximum oil yield observed after 30 min was 96.9 % for vPP and 94.5 % for rPP. However, for longer degradation times, the degradation of rPP results in more solid residues (up to 10 % more than vPP), which is likely due to the various impurities and additives that accumulate in rPP during each successive recycling cycle. The composition of the oil phase differed mainly

in the proportion of aromatic compounds, which was 15.6 % higher for rPP than vPP after 30 min. This may affect the future use of oil product, obtained from different PP materials. The composition of the gas phase produced after the decomposition of vPP and rPP is similar, with C<sub>3</sub> hydrocarbons being the most abundant components representing more than 35 % of the gas phase. Further research could focus on evaluating the applicability of each decomposition product and comparing it to the material from which the product was obtained. The results could help to better understand the hydrothermal degradation processes of PP to oil and gasses after all recycling options have been exhausted, which would lead to a higher recovery of raw and waste materials and help to reduce the disposal of plastic waste.

### Acknowledgments

The authors would like to acknowledge the Slovenian Research Agency (research core funding No. P2-0421 and project No. J7-3149) for financing this research.

### References

- Alsabri A., Tahir F., Al-Ghamdi S.G., 2022, Environmental impacts of polypropylene (PP) production and prospects of its recycling in the GCC region, *Materials Today: Proceedings*, 56(International Conference on Applied Research and Engineering 2021), 2245–2251.
- Anuar Sharuddin S.D., Abnisa F., Wan Daud W.M.A., Aroua, M.K., 2016, A review on pyrolysis of plastic wastes, *Energy Conversion and Management*, 115, 308–326.
- Bai B., Wang, W., Jin H., 2020, Experimental study on gasification performance of polypropylene (PP) plastics in supercritical water, *Energy*, 191, 116527.
- Camacho W., Karlsson, S., 2002, Assessment of thermal and thermo-oxidative stability of multi-extruded recycled PP, HDPE and a blend thereof, *Polymer Degradation and Stability*, 78, 385–391.
- Cecon V.S., Da Silva P.F., Curtzwiler G.W., Vorst K.L., 2021, The challenges in recycling post-consumer polyolefins for food contact applications: A review, *Resources, Conservation and Recycling*, 167, 105422.
- Chen W.T., Jin K., Linda Wang N.H., 2019, Use of supercritical water for the liquefaction of polypropylene into oil, *ACS Sustainable Chemistry & Engineering*, 7, 3749–3758.
- Čolnik M., Kotnik P., Knez Ž., Škerget M., 2022, Chemical recycling of polyolefins waste materials using supercritical water, *Polymers*, 14, 4415.
- European Commission, 2020, Energy, transport and environment statistics: 2020 edition, European Union, Luxembourg.
- Hahladakis J.N., Velis C.A., Weber R., Iacovidou E., Purnell P., 2018, An overview of chemical additives present in plastics: Migration, release, fate and environmental impact during their use, disposal and recycling, *Journal of Hazardous Materials*, 344, 179–199.
- Hamskog M., Klügel M., Forsström D., Terselius B., Gijsman P., 2006, The effect of adding virgin material or extra stabilizer on the recyclability of polypropylene as studied by multi-cell imaging chemiluminescence and microcalorimetry, *Polymer Degradation and Stability*, 91(3), 429–436.
- Jin K., Vozka P., Gentilcore C., Kilaz G., Wang N.H.L., 2021, Low-pressure hydrothermal processing of mixed polyolefin wastes into clean fuels, *Fuel*, 294, 120505.
- Kotnik P., Čolnik M., Finšgar M., Knez Ž., Škerget M., 2020, Determination of C<sub>1</sub>C<sub>6</sub> hydrocarbons in gaseous plastic degradation products by GC–MS method, *Polymer Degradation and Stability*, 182, 109386.
- Laredo G.C., Reza J., Meneses Ruiz E., 2023, Hydrothermal liquefaction processes for plastics recycling: A review, *Cleaner Chemical Engineering*, 5, 100094.
- Olalo A. J., 2021, Characterization of pyrolytic oil produced from waste plastic in Quezon city, Philippines using non-catalytic pyrolysis method, *Chemical Engineering Transactions*, 86, 1495–1500.
- Petrovič A., Čolnik M., Prša A., Fan Y. V., Škerget M., Knez Ž., Klemenš J. J., Čuček L., 2022, Comparative analysis of virgin and recycled thermoplastic polymer based on thermochemical characteristics, *Chemical Engineering Transactions*, 94, 1321–1326.
- Queiroz A., Pedroso G.B., Kuriyama S.N., Fidalgo-Neto A.A., 2020, Subcritical and supercritical water for chemical recycling of plastic waste, *Current Opinion in Green and Sustainable Chemistry*, 25, 100364.
- Seshasayee M.S., Savage P.E., 2020, Oil from plastic via hydrothermal liquefaction: production and characterization, *Applied Energy*, 278, 115673.
- Zhao P., Yuan Z., Zhang J., Song X., Wang C., Guo Q., Ragauskas A.J., 2021, Supercritical water co-liquefaction of LLDPE and PP into oil: properties and synergy, *Sustainable Energy & Fuels*, 5, 575–583.